

Gauss-Bonnet holographic superconductors in Born-Infeld electrodynamics with backreactions

Yunqi Liu, Yan Peng, Bin Wang

INPAC and Department of Physics, Shanghai Jiao Tong University, Shanghai 200240, China

Abstract

We develop a general holographic superconductor away from the probe limit by considering the corrections both in the gravity and in the gauge matter fields. We find the consistent effects of the high curvature correction in the gravity, the nonlinear correction in the gauge matter field and the backreaction on the dynamics of bulk AdS background and boundary CFT. They all have the effect to protect the stability of the bulk spacetime and hinder the formation of the scalar hair condensation on the boundary.

PACS numbers: 11.25.Tq, 04.70.Bw, 74.20.-z

I. INTRODUCTION

The holographic model of superconductors, which is constructed by a gravitational theory of a Maxwell field coupled to a charged complex scalar field via anti-de Sitter/conformal field theory (AdS/CFT) correspondence, has been investigated extensively in the past years (for reviews, see Refs. [1]–[3] and references therein). According to the AdS/CFT correspondence, the emergence of the scalar hair in the bulk AdS black hole corresponds to the formation of a charged condensation in the boundary dual CFTs. This provides a novel way to investigate the superconductor and attracts considerable interest for its potential applications to the condensed matter physics [4–20].

Motivated by the application of the Mermin-Wagner theorem to the holographic superconductors, there have been a lot of interest in generalizing the Einstein gravity background in the holographic superconductor to include the curvature correction in gravity. By examining the charged scalar field together with a Maxwell field in the Gauss-Bonnet-AdS black hole background [7, 19, 21–32], it has been observed that the higher curvature correction makes the condensation harder to form. Other attempts to study the holographic superconductor by modifying gravity background can be found in [33–35].

In the low-energy limit of heterotic string theory, the higher-order correction term also appears in the Maxwell gauge field [36]. Besides the curvature correction to the gravity, it is also interesting to investigate the high-order correction related to the gauge matter field. In the study of the ratio of shear viscosity to entropy density, it was found that the higher derivative correction to the gravity has different effect from that of the higher derivative correction to the gauge matter fields [37]. This motivates people to study the effect of higher order corrected Maxwell field on the scalar condensation and compare with the effect brought by the correction in the gravity [38]. Considering that the Born-Infeld electrodynamics [39] is the only possible non-linear version of electrodynamics which is invariant under electromagnetic duality transformations [40], the nonlinear extension on the gauge field described by the Born-Infeld electrodynamics has been employed in the study on the stability of the bulk spacetime [41] and its influence on the condensation in CFT [20, 42–44]. These studies were concentrated on the background of neutral AdS black holes and in the probe limit approximation.

In the present work we would like to combine the higher order gravity corrections together with the higher corrections to the gauge matter fields in the study of the holographic superconductor and compare their effects

on the condensation. We will examine the holographic superconductor away from the probe approximation and take the backreaction of the spacetime into account. Considering the backreaction of classical fields onto the spacetime is not trivial. In [41] it was found that the nonzero backreaction can make the neutral AdS black hole become Born-Infeld AdS black hole. In our work, considering the backreaction, we will obtain the Gauss-Bonnet Born-Infeld AdS black hole in the gravity side and we will examine the condensation of the scalar field in this background when it is coupled with the Born-Infeld electromagnetic field. We will present a complete picture of the holographic superconductor with corrections in the gravity side together with the gauge matter fields and take the backreaction into account.

The outline of this work is as follows. In section II, we will introduce the model, derive the set of equations of motion. In section III we will study the dynamics of a scalar perturbation in the high temperature phase. In section IV we will show the effect of the backreaction, Gauss-Bonnet factor and the Born-Infeld factor on the condensate. In section V, we will analyze the conductivity of the holographic superconductor. We will conclude our main results in the last section.

II. ACTION AND THE EQUATIONS OF MOTION

The general action describing the Born-Infeld field and a charged complex scalar field in the five-dimensional Einstein-Gauss-Bonnet spacetime with negative cosmological constant reads

$$S = \frac{1}{2\kappa^2} \int d^5x \sqrt{-g} \left[R + \frac{12}{l^2} + \frac{\alpha}{2} (R^{abcd} R_{abcd} - 4R^{ab} R_{ab} + R^2) \right] \\ + \int d^5x \sqrt{-g} \left[\frac{1}{b^2} \left(1 - \sqrt{1 + \frac{b^2 F^{ab} F_{ab}}{2}} \right) + (-|\nabla\Psi - iqA\Psi|^2 - m^2|\Psi|^2) \right], \quad (1)$$

where κ is the five dimensional gravitational constant $\kappa^2 = 8\pi G_5$ with G_5 the five-dimensional Newton constant, g is the determinant of the metric, l here is the AdS radius, q and m are respectively the charge and the mass of the scalar field. b is the Born-Infeld coupling parameter. In the limit $b \rightarrow 0$, the Born-Infeld field will reduce to the Maxwell field.

When there is no backreaction of classical fields onto the spacetime, we have the Gauss-Bonnet AdS black hole on the gravity background with the metric

$$ds^2 = -f(r)dt^2 + \frac{dr^2}{f(r)} + \frac{r^2}{l_e^2} (dx^2 + dy^2 + dz^2), \quad (2)$$

where

$$f(r) = \frac{r^2}{2\alpha} \left[1 - \sqrt{1 - \frac{4\alpha}{l^2} \left(1 - \frac{r_h^4}{r^4} \right)} \right], \quad (3)$$

and

$$l_e^2 = \frac{l^2}{2} \left[1 + \sqrt{1 - \frac{4\alpha}{l^2}} \right] \quad (4)$$

is the effective AdS radius. The Hawking temperature of the Gauss-Bonnet AdS black hole, which will be interpreted as the temperature of the CFT, can be expressed as

$$T = \frac{f'(r)}{4\pi} \Big|_{r=r_h} . \quad (5)$$

We will consider the backreaction in our work, thus we take a metric ansatz of the gravitational background in the form

$$ds^2 = -f(r)e^{-\chi(r)}dt^2 + \frac{dr^2}{f(r)} + \frac{r^2}{l_e^2}(dx^2 + dy^2 + dz^2) . \quad (6)$$

The electromagnetic field and the scalar field can be chosen as

$$A_t = \phi(r)dt, \quad \Psi = \Psi(r), \quad (7)$$

where $\Psi(r)$ can be taken to be real without loss of generality. The Hawking temperature of this black hole is changed to be

$$T = \frac{f'(r)e^{-\chi(r)/2}}{4\pi} \Big|_{r=r_h} . \quad (8)$$

Considering the ansatz of the metric when we take into account the backreaction, the equations of motions can be obtained

$$\begin{aligned} 0 &= \psi''(r) + \psi'(r) \left[\frac{3}{r} + \frac{f'(r)}{f(r)} - \frac{\chi'(r)}{2} \right] + \psi(r) \left[\frac{q^2\phi(r)^2 e^{\chi(r)}}{f(r)^2} - \frac{m^2}{f(r)} \right], \\ 0 &= \left[\phi''(r) + \left(\frac{\chi'(r)}{2} + \frac{3}{r} \right) \phi'(r) \right] (1 - b^2 e^{\chi(r)} \phi'(r)^2) + \frac{b^2}{2} \phi'(r) e^{\chi(r)} [\chi'(r) \phi'(r)^2 \\ &\quad + 2\phi'(r) \phi''(r)] - \frac{2q^2\phi(r)\psi(r)^2}{f(r)} (1 - b^2 e^{\chi(r)} \phi'(r)^2)^{\frac{3}{2}}, \\ 0 &= (1 - \frac{2\alpha f(r)}{r^2}) \chi'(r) + \frac{4}{3} \kappa^2 r \left[\frac{q^2\phi(r)^2 \psi(r)^2 e^{\chi(r)}}{f(r)^2} + \psi'(r)^2 \right], \\ 0 &= (1 - \frac{2\alpha f(r)}{r^2}) f'(r) + \frac{2}{r} f(r) - \frac{4r}{l^2} + \frac{2}{3} \kappa^2 r \left[\left(\frac{q^2\phi(r)^2 \psi(r)^2 e^{\chi(r)}}{f(r)} + f(r) \psi'(r)^2 + m^2 \psi(r)^2 \right. \right. \\ &\quad \left. \left. \frac{e^{\chi(r)} q^2 \phi(r)^2 \psi(r)^2}{f(r)} \right) + \frac{1}{b^2} \left[(1 - b^2 \phi'(r)^2)^{-1/2} - 1 \right] \right], \end{aligned} \quad (9)$$

where the prime denotes the derivative with respect to r .

There are two branches of solutions to the above equations Eq.(9), which are classified into high temperature solutions and low temperature solutions. In the following we will provide detailed discussions on these two branches of solutions.

III. DYNAMICS AT HIGH TEMPERATURE PHASE

In this part, we will mainly discuss the solutions of the above equations of motions when the black hole temperature is high.

Using the separation $\psi_{\omega, k}(r)e^{-i(\omega t + kx)}$, we can rewrite the perturbation equation of the scalar field with mass in the background (6) into

$$0 = \psi''_{\omega, k}(r) + \psi'_{\omega, k}(r) \left[\frac{3}{r} + \frac{f'(r)}{f(r)} - \frac{\chi'(r)}{2} \right] + \psi_{\omega, k}(r) \left\{ \frac{[\omega + q\phi(r)]^2 e^{\chi(r)}}{f(r)^2} - \frac{m^2}{f(r)} - \frac{l^2 k^2}{f(r)r^2} \right\}. \quad (10)$$

When the scalar perturbation settles down, the Einstein equations in Eq.(9) are reduced to

$$\begin{aligned} 0 &= \left(1 - \frac{2\alpha f(r)}{r^2} \right) f'(r) + \frac{2f(r)}{r} - \frac{4r}{l^2} + \frac{2}{3b^2} \kappa^2 r \left[(1 - b^2 \phi'(r)^2)^{-1/2} - 1 \right], \\ 0 &= \left(1 - \frac{2\alpha f(r)}{r^2} \right) \chi'(r), \end{aligned} \quad (11)$$

and the equation governing the electromagnetic field becomes

$$0 = \left[\phi''(r) + \left(\frac{\chi'(r)}{2} + \frac{3}{r} \right) \phi'(r) \right] (1 - b^2 e^{\chi(r)} \phi'(r)^2) + \frac{b^2}{2} \phi'(r)^2 e^{\chi(r)} (\chi'(r) \phi'(r) + 2\phi''(r)). \quad (12)$$

We can do the rescales in Eq.(10), (11) and (12)

$$e^{\chi} \rightarrow a^2 e^{\chi}, \quad \phi \rightarrow a^{-1} \phi, \quad t \rightarrow at, \quad \omega \rightarrow a^{-1} \omega, \quad (13)$$

$$l \rightarrow al, \quad \alpha \rightarrow a^2 \alpha, \quad \omega \rightarrow a^{-1} \omega, \quad r \rightarrow ar, \quad q \rightarrow q/a, \quad m^2 \rightarrow m^2/a^2, \quad b^2 \rightarrow a^2 b^2, \quad k \rightarrow a^{-1} k \quad (14)$$

$$r \rightarrow ar, \quad f \rightarrow a^2 f, \quad \phi \rightarrow a\phi, \quad \omega \rightarrow a\omega, \quad (15)$$

$$q \rightarrow aq, \quad \phi \rightarrow a^{-1} \phi, \quad \kappa^2 \rightarrow \kappa^2 a^2, \quad b^2 \rightarrow a^2 b^2. \quad (16)$$

The first rescale guarantees $\chi(r) = 0$, the second one sets AdS radius as unity. Using the third rescale, we can set $r_h = 1$. The last rescale relates the parameter of the backreaction κ^2 to the charge of the scalar field q . From (16), we can see that, as κ^2 is fixed the increase of q corresponds to the decrease of κ^2 with fixed q . Thus when κ^2 is fixed, a larger q leads to weaker backreaction.

Substituting $\chi(r) = 0$, Eq.(12) becomes

$$0 = b^2 \phi'(r)^2 \phi''(r) + (1 - b^2 \phi'(r)^2) \left(\frac{3\phi'(r)}{r} + \phi''(r) \right), \quad (17)$$

which provides the analytical solution [45, 46]

$$\phi(r) = U + \frac{Q}{r^2} {}_2F_1\left[\frac{1}{3}, \frac{1}{2}, \frac{4}{3}, -\frac{4b^2Q^2}{r^6}\right], \quad (18)$$

where Q and U are integral constants. U can be eliminated by the constraint at the horizon, $\phi(r_h) = 0$,

$$U = -Q {}_2F_1\left[\frac{1}{3}, \frac{1}{2}, \frac{4}{3}, -4b^2Q^2\right].$$

At infinity, Eq.(18) asymptotically behaves as

$$\phi(r) \sim U - \frac{Q}{r^2}.$$

In the limit $b \rightarrow 0$, Eq.(17) is reduced to

$$0 = \frac{3\phi'(r)}{r} + \phi''(r) \quad (19)$$

which is the equation of motion of the electromagnetic field in the Maxwell theory. The solution reads

$$\phi(r) = Q - \frac{Q}{r^2}.$$

Substituting Eq.(18) into Eq.(11), the gravitational field equation is rewritten as

$$0 = \left(1 - \frac{2\alpha f(r)}{r^2}\right) f'(r) + \frac{2f(r)}{r} - \frac{4r}{l^2} - \frac{2\kappa^2 r}{3b^2} + \frac{2\kappa^2}{3b^2 r^2} \sqrt{4b^2 Q^2 + r^6}, \quad (20)$$

which has an analytical solution [47, 48]

$$f(r) = \frac{r^2}{2\alpha} (1 - \sqrt{g(r)}), \quad (21)$$

where the function $g(r)$ is

$$g(r) = 1 - \frac{4\alpha}{l^2} + \frac{4\alpha\tilde{m}}{r^4} - \frac{\kappa^2\alpha}{3b^2} + \frac{\kappa^2\alpha}{3b^2 r^3} \sqrt{r^6 + 4b^2 Q^2} - \frac{2\alpha\kappa^2 Q^2}{r^6} {}_2F_1\left[\frac{1}{3}, \frac{1}{2}, \frac{4}{3}, -\frac{4b^2 Q^2}{r^6}\right]. \quad (22)$$

${}_2F_1$ represents a hypergeometric function, Q is an integral constant which actually plays the role of electric charge of the black hole and \tilde{m} is an integral constant relating to the black hole ADM mass. In the limit of vanishing Gauss-Bonnet factor, the background spacetime reduces to a Born-Infeld AdS black hole [45]. If we take the limit $b \rightarrow 0$, the background spacetime reduces to a Gauss-Bonnet Reissner Nordstrom AdS black hole. There is an upper bound of the electric charge Q_c contained inside the black hole, which indicates the phase transition point of the black hole. Beyond Q_c , the black hole will become unstable. This Q_c has to be calculated numerically for the Gauss-Bonnet Born-Infeld AdS black hole.

In order to investigate the scalar perturbation Eq.(10), near the horizon $r \sim 1$, we should impose the incoming wave boundary condition

$$\psi_{\omega,k}(r) \sim (r-1)^{-i\frac{\omega}{4\pi T}}. \quad (23)$$

Introducing a new variable φ as $\psi_{\omega,k}(r) = \mathfrak{R}(r)\varphi_{\omega,k}(r)$ and choosing $\mathfrak{R}(r) = \exp[-i \int_1^r \frac{\omega + q\phi(r)}{f(r)}]$, which asymptotically approaches Eq.(23) at the horizon, one can express the boundary condition at the horizon as $\varphi_{\omega,k}|_{r=1} = \text{const.}$, and Eq. (10) then becomes

$$0 = \varphi''_{\omega,k}(r) + B_1(r)\varphi'_{\omega,k}(r) + B_2(r)\varphi_{\omega,k}(r), \quad (24)$$

with

$$\begin{aligned} B_1(r) &= \frac{f'(r)}{f(r)} - \frac{2i[q\phi(r) + \omega]}{f(r)} + \frac{3}{r}, \\ B_2(r) &= -\frac{m^2}{f(r)} - \frac{k^2}{r^2 f(r)} - \frac{i[3(q\phi(r) + \omega) + r\phi'(r)]}{rf(r)}. \end{aligned} \quad (25)$$

Near the AdS boundary $r \sim \infty$, $\varphi_{\omega,k}$ behaves as

$$\varphi_{\omega,k}(r) \sim \frac{\varphi_{\omega,k}^-}{r^{\lambda_-}} + \frac{\varphi_{\omega,k}^+}{r^{\lambda_+}}. \quad (26)$$

where $\lambda_{\pm} = 2 \pm \sqrt{4 + m^2 l_e^2}$ are characteristic exponents of the perturbation equation, and l_e^2 is the effective AdS radius. The boundary conditions at the horizon are now given by

$$\begin{aligned} \varphi_{\omega,k}|_{r=1} &= 1, \\ \frac{\varphi'_{\omega,k}}{\varphi_{\omega,k}} \Big|_{r=1} &= - \frac{B_2(r)}{B_1(r)} \Big|_{r=1}. \end{aligned} \quad (27)$$

Eq. (24) is a linear equation and $\varphi_{\omega,k}(r)$ must be regular at the horizon. Since we do not concentrate on the amplitude of $\varphi_{\omega,k}(r)$, we can set $\varphi_{\omega,k}|_{r=1} = 1$. Eq. (24) has to be solved numerically under the boundary conditions (27) and $\varphi_{\omega,k}^- = 0$ at infinity.

We will examine the behavior of the charged scalar field perturbation which can present us an objective picture on how the black hole evolves when the temperature drops and when the backreaction becomes stronger. Without loss of generality, hereafter we will set $m^2 = -3/l^2$ in our calculation.

A. Dynamical behavior of the scalar perturbation in the bulk

Hereafter we will report dynamical perturbation and critical phenomenon. We will pay more attention on how the Born-Infeld factor, the Gauss-Bonnet factor and the backreaction influence the perturbation in the

bulk background spacetime when the temperature of the black hole drops. Further we are going to study the critical phenomenon once the black hole approaches marginally stable.

For the scalar perturbation, we will concentrate on the lowest quasinormal mode as studied in [49–52]. We can obtain the quasinormal frequencies by solving Eq.(24) based on the boundary conditions (27) at the horizon and $\varphi_{\omega,k=0}^- = 0$ at the AdS boundary. For a stable spacetime, the outside perturbation will exhibit a decay mode. When the perturbation grows up, the background spacetime becomes unstable.

As the background spacetime approaches marginally stable and finally changes to be unstable, the black hole will experience a phase transition. The correlation length is the scale parameter that exists in the system near the phase transition point. It increases while the temperature approaches its critical value and becomes infinite at the moment of the phase transition. The correlation length is defined as $\xi^2 := -k^{-2}$ [19] and can be calculated by solving Eq. (24) with $\omega = 0$ under boundary conditions Eq. (27) at the horizon and $\varphi_{\omega=0,k}^- = 0$ at the AdS boundary.

Let us first see the influence on the quasinormal modes and correlation length given by the Born-Infeld factor. To illustrate the influence, we set a vanishing Gauss-Bonnet factor and fix the backreaction parameter $\kappa^2 = 0.05$. In the left panel of Fig.1 we show the dependence of the imaginary part of quasinormal frequency on the Born-Infeld factor b . With the increase of the electric charge of the black hole Q , the imaginary part of the quasinormal frequency approaches zero monotonously. When $Q < Q_c$, the imaginary part of the frequency keeps negative, which shows that the perturbation has a decay mode ensuring the stable spacetime. For the fixed Q , we observe that a bigger value of the Born-Infeld factor b leads to bigger absolute value of the imaginary part of the quasinormal frequency. Considering that the decay time scale of the perturbation $\tau \sim 1/|IM(\omega)|$, bigger b will make the perturbation decay faster. This means that the stronger nonlinearity in the electromagnetic field can make the perturbation die out quicker and protect the background spacetime to be more stable.

The influence of Born-Infeld factor b on the correlation length is shown in the right panel of Fig. 1. As Q tends to its critical value Q_c , the correlation length approaches infinity. A larger b slows down the process to make ξ infinity, which implies that the black hole background is more stable when b is bigger. This is consistent with the observation in the quasinormal modes behavior.

Now we turn to exhibit the influence of the Gauss-Bonnet factor on the perturbation in the background of Gauss-Bonnet Born-Infeld AdS black hole. We fix the backreaction factor κ^2 and the Born-Infeld factor b to be 0.05 and 0.14, respectively, in our numerical calculation. As shown in Fig.2, the imaginary part of

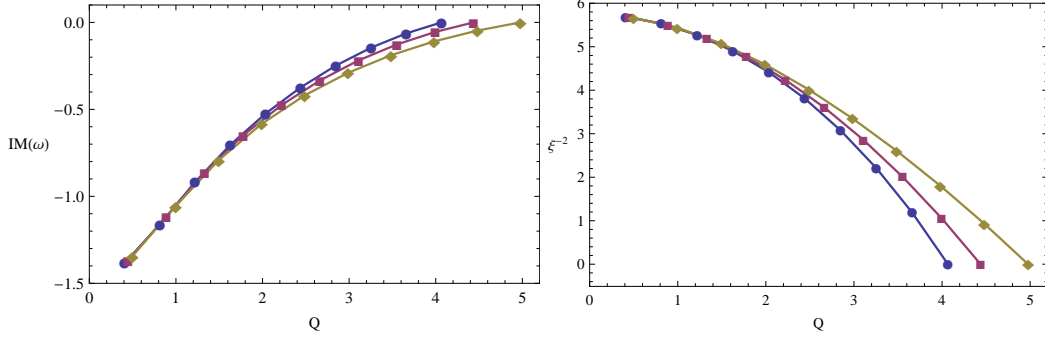


FIG. 1: (Color online) Left) The imaginary part of the lowest quasinormal frequency for different values of b when κ^2 and α are fixed to be 0.05 and 0 respectively. Lines from top to bottom correspond to $b = 0.05, 0.1$ and 0.14 , respectively. Right) The correlation length ξ as a function of Q for different values of b . Lines from bottom to top correspond to $b = 0.05, 0.1$ and 0.14 , respectively.

quasinormal frequency keeps approaching zero with the increase of the black hole charge Q . For the fixed black hole charge, we observe that when the Gauss-Bonnet factor α is bigger, the absolute value of the imaginary part of the quasinormal frequency becomes bigger. This tells us that the bigger Gauss-Bonnet factor makes the perturbation decay quicker, which corresponds to say that the bigger α can keep to background spacetime to be more stable.

The dependence of correlation length of scalar perturbation on the Gauss-Bonnet factor is shown in the right panel of Fig.2. As the electric charge of black holes approach their critical values, the correlation length keeps increasing to infinity. A larger α can slow down the process to make ξ infinity, which means that more curvature correction can delay the system to approach the phase transition point. This is consistent with the quasinormal behavior, indicating that the background is more stable when the α is bigger.

From the above results, we find that the higher order gravity correction and the higher correction to the gauge matter field basically play the same role in the perturbation in the background Gauss-Bonnet Born-Infeld AdS black hole. Both of them can protect the spacetime to be away from instability.

In order to investigate the influence of the backreaction, one has to fix κ^2 , say $\kappa^2 = 1$, and study how the parameter q affects the behavior of the scalar perturbation. Using the rescale (16) to set $q = 1$ will change Q in different scale for various strength of the backreaction. It is worth noting that the larger the q is, the weaker the backreaction is. Fig. 3 shows the dependence of perturbation frequency and correlation length with the change of the coupling q while backreaction κ^2 , Born-Infeld factor b and Gauss-Bonnet factor α are fixed to be 1, 0.1 and 0 respectively. The frequencies of the scalar perturbation approach zero as the electric charge approaches to its critical value. The stronger coupling q makes $IM(\omega)$ approach zero quicker. This indicates that the black hole background is easier to be destroyed when the backreaction is weaker and it is more stable

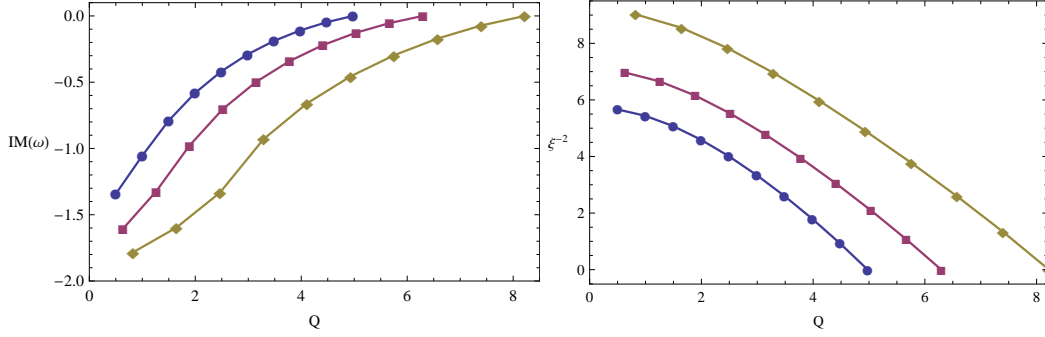


FIG. 2: (Color online) Left) The imaginary part of the lowest quasinormal frequency for different values of α while b^2 and κ^2 are fixed to be 0.02 and 0.05 respectively. Lines from top to bottom correspond to $\alpha = 0, 0.1$ and 0.2 , respectively. Right) The correlation length ξ as a function of Q for different values of α . Lines from bottom to top correspond to $\alpha = 0, 0.1$ and 0.2 , respectively.

when the backreaction is stronger. The behavior of the correlation length further supports this result. The weaker coupling q (stronger backreaction) makes ξ increase slower, which shows that the background is more stable as the backreaction increases.

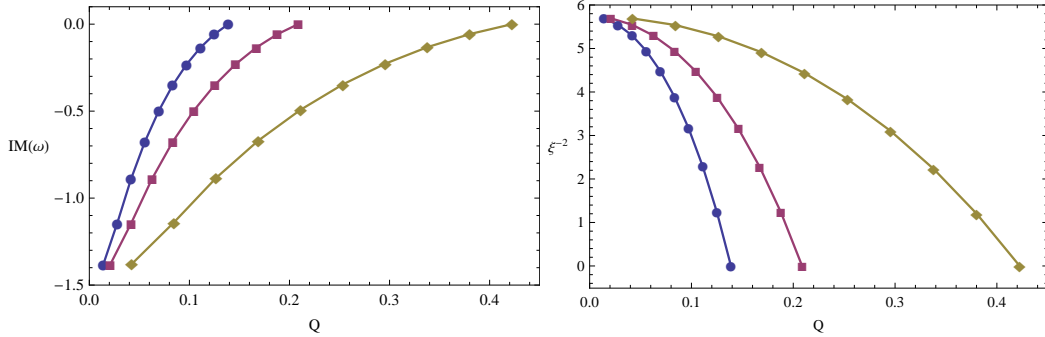


FIG. 3: (Color online) Left) The imaginary parts of the lowest quasinormal frequency for different values of q while κ^2, b and α are fixed to be 1, 0.1 and 0 respectively. Lines from bottom to top correspond to $q = 10, 20$ and 30 , respectively. Right) The correlation length ξ as a function of Q for different q . Line from top to bottom correspond to $q = 10, 20$ and 30 , respectively.

B. The critical temperature in the bulk spacetime and its dependence on Gauss-Bonnet and Born-Infeld parameters

The charge density Q determines the phase structure. When we fix parameters κ^2, b, α and q , the critical value of the black hole charge Q_c indicates the starting point of the phase transition. This Q_c can be obtained by solving Eq.(24) with $\omega = k = 0$ under the boundary condition at the horizon and $\varphi_{\omega=0, k=0}^- = 0$ at infinity using the shooting method. Inserting the value of Q_c into the Hawking temperature, we can obtain the critical temperature T_c in the bulk black hole spacetime.

In the following two tables, I and II, we list the values of T_c in a Gauss-Bonnet Born-Infeld AdS black hole described by Eq.(8) with different values of parameters. From table I we can see that T_c decreases with

the increase of the Born-Infeld factor regardless of the choices of the Gauss-Bonnet factor. In table II, the Born-Infeld factor is fixed as 0.14, we find that T_c decreases with the increase of α . This shows that both the higher order gravity correction and the higher correction to the gauge matter field can make the critical temperature smaller, which ensures the black hole background to be more stable.

TABLE I: The dependence of the critical temperature $T_c/Q_c^{\frac{1}{3}}$ on b for different values α . We set $q = 1$, $\kappa^2 = 0.05$ and $m^2 l^2 = -3$ in our numerical computation.

$\alpha \backslash b$	1/20	1/10	$\sqrt{2}/10$
0	0.147	0.139	0.130
1/10		0.110	0.0976

TABLE II: The dependence of the critical temperature $T_c/Q_c^{\frac{1}{3}}$ on the Gauss-Bonnet factor α . We set $q = 1$, $\kappa^2 = 0.05$, $b = 0.14$ and $m^2 = -3/l^2$ in the numerical computation.

α	-0.1	0	0.1	0.15	0.2
$T_c/Q_c^{\frac{1}{3}}$	0.156	0.130	0.0976	0.0782	0.0571

IV. SOLUTIONS AT LOW TEMPERATURE PHASE

When the black hole temperature drops to T_c , we observed that the imaginary part of the quasinormal frequency will change from negative to zero, which means that a stable black hole background will become marginally stable. When $T \sim T_c$, the original Gauss-Bonnet Born-Infeld AdS black hole spacetime will be destroyed and a new configuration with scalar hair will be formed. In order to study the condensation of the scalar hair, we will use the shooting method to solve the equations of motions (9) numerically with appropriate boundary conditions.

At the black hole horizon r_h , which is the root of $f(r_h) = 0$, the solutions of the gauge and the scalar fields have to be regular

$$\phi(r_h) = 0, \quad \psi'(r_h) = \frac{m^2}{f'(r_h)} \psi(r_h), \quad (28)$$

and the coefficients in the metric ansatz obey

$$f'(r_h) = \frac{4r_h}{l^2} - \frac{2}{3}\kappa^2 r_h \left[m^2 \psi(r_h)^2 \frac{e^{\chi(r)} q^2 \phi(r)^2 \psi(r)^2}{f(r)} + \frac{1}{b^2} \left[(1 - b^2 \phi'(r_h)^2)^{-1/2} - 1 \right] \right], \quad (29)$$

$$\chi'(r_h) = -\frac{4}{3}\kappa^2 r_h \left[\frac{q^2 \phi'(r_h)^2 \psi(r_h)^2 e^{\chi(r_h)}}{f'(r_h)^2} + \psi'(r_h)^2 \right]. \quad (30)$$

At the spatial infinity, the asymptotic behaviors of the solutions are

$$\begin{aligned} \chi &\rightarrow 0, \quad f(r) \sim \frac{r^2}{l^2}, \\ \phi(r) &\sim \mu - \frac{\rho}{r^2}, \quad \psi(r) \sim \frac{\psi_-}{r^{\lambda_-}} + \frac{\psi_+}{r^{\lambda_+}}, \end{aligned} \quad (31)$$

where $\lambda_{\pm} = 2 \pm \sqrt{4 + m^2 l_e^2}$, μ is the chemical potential. We choose $\psi_- = 0$, thus one can interpret $\langle \mathcal{O}_{\lambda+} \rangle = \psi_+$, where $\mathcal{O}_{\lambda+}$ is the operator with the conformal dimension $\lambda+$ dual to the scalar field.

There are several scaling symmetries to be adopted in the above equations as those in [6, 26]

$$e^{\chi} \rightarrow a^2 e^{\chi}, \quad \phi \rightarrow \phi/a, \quad t \rightarrow at, \quad (32)$$

$$l \rightarrow al, \quad \alpha \rightarrow a^2 \alpha, \quad r \rightarrow ar, \quad q \rightarrow q/a, \quad m^2 \rightarrow m^2/a^2, \quad b^2 \rightarrow a^2 b^2, \quad (33)$$

$$r \rightarrow ar, \quad f \rightarrow a^2 f, \quad \phi \rightarrow a\phi, \quad (34)$$

$$q \rightarrow aq, \quad \phi \rightarrow \phi/a, \quad \psi \rightarrow \psi/a, \quad \kappa^2 \rightarrow \kappa^2 a^2, \quad b^2 \rightarrow a^2 b^2. \quad (35)$$

We can use symmetry (32) to set the asymptotic value of χ to zero. Employing symmetry (33), we have $l = 1$. Further using symmetries (34), (35), we get $r_h = 1$ and $q = 1$.

The behavior of the holographic superconductor can be found by numerically integrating Eq.(9) with the appropriate boundary conditions Eq.(28)-Eq.(31) at the horizon and the AdS boundary.

In the following we will discuss the scalar condensation in the holographic superconductor and disclose its dependence on the parameters of the backreaction, Gauss-Bonnet factor and Born-Infeld factor. The numerical computation allows a full exploration of the condensation of the scalar field $\langle \mathcal{O}_{\lambda+} \rangle$.

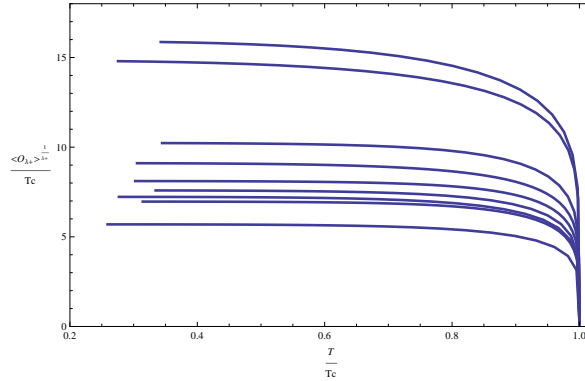


FIG. 4: Dependence of the scalar condensate on various parameters.

The dependence of the scalar condensation on various parameters is shown in fig.4. For the convenience of the following discussion, we number lines from bottom to top in fig.4 in the order of 1 to 9. The physics

parameters of each line are listed in Table III. We observe that when the condensation gap becomes bigger, the critical temperature to start the condensation becomes smaller, which means that it is more difficult for the scalar hair to condense. The critical temperature for the condensation of the scalar operator calculated in CFT coincides with that reported in tables I and II from the analysis of the spacetime stability in the bulk. This gives further evidence of the holography.

TABLE III: This table provide the characteristic parameter of each line in Fig.4. The lines in Fig.4 have been labeled from 1 to 9 from bottom to top.

<i>line</i>	1	2	3	4	5	6	7	8	9
$T_c/\rho^{\frac{1}{3}}$	0.189	0.156	0.147	0.139	0.130	0.110	0.0976	0.0582	0.0571
α	0	-0.1	0	0	0	0.1	0.1	0.1	0.2
κ^2	0	0.05	0.05	0.05	0.05	0.05	0.05	0.1	0.05
b	0.1	0.14	0.05	0.1	0.14	0.1	0.14	0.14	0.14

We now discuss the dependence of the condensation on various parameters. In lines 3, 4, and 5, we take the same values of the Gauss-Bonnet factor and the strength of the backreaction, namely $\alpha = 0, \kappa^2 = 0.05$, we see that the condensation gap increases as the Born-Infeld factor increases. This means that the scalar condensation becomes harder to be formed when the nonlinearity in the electromagnetic field increases. This agrees with the observation that the stability is kept well with the highly nonlinear electromagnetic field observed in the bulk dynamics study. This property also holds when we compare lines 6 and 7.

If we look at lines 2, 5, 7 and 9, where the strength of the backreaction and the Born-Infeld factor are fixed to be $\kappa^2 = 0.05, b = 0.14$, we observe that the condensation gap increases with the increase of the Gauss-Bonnet factor. Comparing with the result in [21], we find that the higher order gravity correction influence on the condensation will not be changed when the scalar field is coupled to the nonlinear electromagnetic field. The Gauss-Bonnet factor will make the condensation harder for the scalar field no matter whether the scalar field is coupled to a linear or nonlinear gauge matter field.

The effect on the condensation brought by the backreaction is similar to the corrections in gravity and gauge matter field. The condensation gap increases when the backreaction becomes stronger, which indicates that the condensation becomes harder to form when there is stronger backreaction from the matter fields to the gravity. This is also consistent with the observation in the background stability analysis.

The influences given by the Born-Infeld, Gauss-Bonnet and backreaction factors can be further understood

by examining the effective mass of the scalar field, which is expressed as

$$m_{eff}^2 = m^2 + q^2 A_t^2 g^{tt}(r) = -\frac{3}{l^2} - \frac{\phi^2(r)}{f(r)} e^{\chi(r)}. \quad (36)$$

$g^{tt}(r)$ is negative, so there is a chance that the effective mass becomes sufficiently negative near the horizon to destabilize the scalar field. From Fig.5 we observe that with the growth of the Born-Infeld factor and the strength of the backreaction, the effective mass develops a more shallow well out of the horizon. Similar phenomenon also happens when we increase the Gauss-Bonnet factor. The negative effective mass is the crucial effect to cause the formation of the scalar hair and the less negative effective mass will make it harder for the scalar hair to form [4]. This picture explains the reason why the stronger backreaction, the bigger corrections in gravity and gauge matter field can make the scalar condensation develop harder.

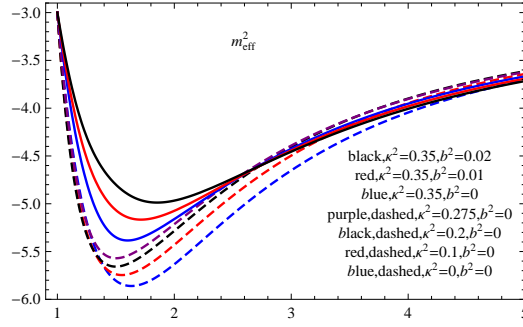


FIG. 5: The dependence of m_{eff}^2 on different parameters with $\psi_+ = 4$ in all the plots.

V. CONDUCTIVITY

In order to investigate the influences of the backreaction, the Born-Infeld factor and the Gauss-Bonnet factor on the conductivity, we consider the time-dependent perturbations with zero momentum $A_i(t, r, x^i) = A(r)e^{-i\omega t}e_i$ and $h_{ti}(t, r, x^i) = h_{ti}(r)e^{-i\omega t}$, where A_i is the perturbation of the vector potential which has only spatial components and $h_{ti}(t, r, x^i)$ is the perturbation of the metric tensor. After some algebra, we obtain the linear equation of motion.

The perturbation equation for $A(r)$ reads

$$\begin{aligned} & -r\phi'(r)e^{\frac{\chi(r)}{2}} \left[h'_{ti}(r) - \frac{2}{r}h_{ti}(r) \right] \\ &= \left[e^{-\frac{\chi(r)}{2}} r f(r) A'(r) \right]' + \frac{A(r)e^{\frac{\chi(r)}{2}} \omega^2 r}{f(r)} - 2q^2 r \psi(r)^2 A(r) e^{-\frac{\chi(r)}{2}} \left[1 - b^2 e^{\chi(r)} \phi'(r)^2 \right]^{\frac{1}{2}} \\ & \quad - \frac{1}{2} b^2 r e^{\frac{\chi(r)}{2}} A'(r) f(r) \left[\phi'(r)^2 \chi'(r) + 2\phi'(r)\phi''(r) \right] \left[1 - b^2 e^{\chi(r)} \phi'(r)^2 \right]^{-\frac{1}{2}}. \end{aligned} \quad (37)$$

The perturbation equation for $h_{ti}(r)$ has the form

$$\left[1 - b^2 \phi'(r)^2 e^{\chi(r)}\right]^{\frac{1}{2}} \left[h'_{ti}(r) - \frac{2}{r} h_{ti}(r) \right] + \frac{2\kappa^2 r^2 A(r) \phi'(r)}{r^2 - 2\alpha f(r)} = 0. \quad (38)$$

By substituting the above equation into Eq.(37), we have

$$\begin{aligned} 0 = & \frac{1}{2} b^2 e^{\chi(r)} A'(r) [\phi'(r)^2 \chi'(r) + 2\phi'(r)\phi''(r)] + [1 - b^2 e^{\chi(r)} \phi'(r)^2] \left[A''(r) + A'(r) \left[\frac{f'(r)}{f(r)} - \frac{\chi'(r)}{2} + \frac{1}{r} \right] \right. \\ & \left. + \frac{\omega^2 A(r) e^{\chi(r)}}{f(r)^2} \right] - A(r) \left[\frac{2\kappa^2 r^2 e^{\chi(r)} \phi'(r)^2 [1 - b^2 e^{\chi(r)} \phi'(r)^2]^{\frac{1}{2}}}{f(r) [r^2 - 2\alpha f(r)]} + \frac{2q^2 \psi(r)^2 [1 - b^2 e^{\chi(r)} \phi'(r)^2]^{\frac{3}{2}}}{f(r)} \right] \end{aligned} \quad (39)$$

This equation is solved under the boundary condition of incoming wave at horizon

$$A(r) \sim f(r)^{-i \frac{\omega}{4\pi T_+}}, \quad (40)$$

where T_+ is the temperature of the (*hairly*) black hole. At infinity the asymptotic behavior of $A(r)$ is

$$A(r) = a_0 + \frac{a_2}{r^2} + \frac{a_0 l_e^4 \omega^2}{2r^2} \log \frac{r}{l}, \quad (41)$$

where a_0 and a_2 are integration constants. Then the conductivity is found to be[23]

$$\sigma = \frac{2a_2}{i\omega L_2^4 a_0} + \frac{i\omega}{2} - i\omega \log\left(\frac{l_e}{l}\right). \quad (42)$$

In the following figures we show the numerical results of conductivity and its dependence on different parameters. The blue line represents the real part and the purple line shows the imaginary part of σ at temperature $T/T_c \simeq 0.32$.

We observe that the influence of the Gauss-Bonnet factor still keeps the same as that disclosed in [21] when the gauge matter field is not the usual Maxwell field. With the increase of the Gauss-Bonnet coupling constant, the gap frequency becomes larger. The nonlinearity in the gauge field does not change this property. With the increase of the Born-Infeld factor, we observe that the conductivity gap frequency becomes larger as well. Thus the higher order gravity correction and the higher correction to the gauge matter field basically play the same role in the conductivity. Similar influence has also been found for the blackreaction.

VI. CONCLUSIONS

In this work we have studied a general picture of holographic superconductor. We have considered high curvature correction in the gravity side and nonlinear correction in the gauge matter field. Instead of the probe limit, we have taken the backreaction of classical fields onto the spacetime into account. With the backreaction, we have obtained the Gauss-Bonnet Born-Infeld AdS black hole. We have analyzed the dynamics

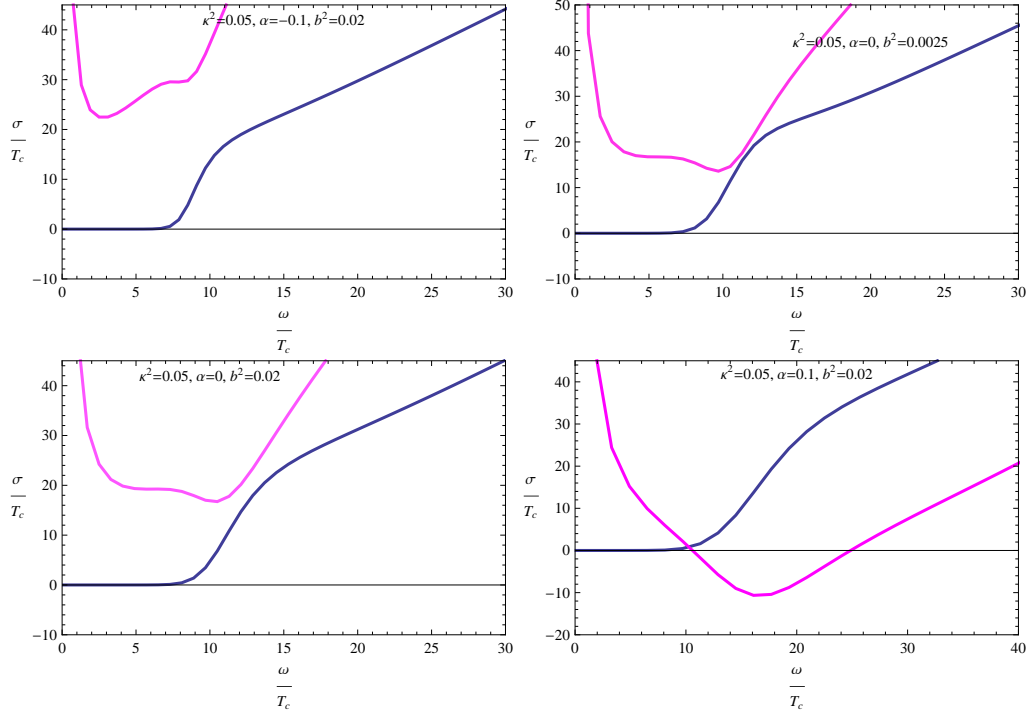


FIG. 6: Influence on the conductivity caused by the Gauss-Bonnet factor and the Born-Infeld factor.

of this gravitational background in the bulk and examined the condensation of the scalar hair in the boundary CFT.

We have obtained the consistent result that the correction in the gravity can make the bulk background more stable and the scalar hair condensation on the boundary more difficult to develop. This property always holds no matter whether the scalar field is coupled to a Maxwell field or a nonlinear electromagnetic field. Furthermore we found that in addition to the neutral AdS black hole background, in the more general configuration such as a nonlinearly charged Gauss-Bonnet AdS black hole, the nonlinear correction in the gauge matter field persists the similar effect in the background stability and condensation of scalar field to that of the correction in the gravity side. The nonlinearity of the electromagnetic field can protect the stability of the background spacetime and make the scalar hair condensation hard to form on the boundary. The consistent effect brought by the corrections in gravity and gauge matter field is different from that observed in calculating the ratio of shear viscosity to entropy density in the AdS background [37]. The reason behind this difference needs to be clarified. The strength of the backreaction plays the similar role to the corrections in gravity and gauge matter field on the spacetime stability and scalar hair formation. The consistent influences of the strength of the backreaction and corrections in gravity and gauge matter field have also been disclosed in the effective mass of the scalar field and the conductivity.

Acknowledgments

This work was partially supported by the National Natural Science Foundation of China.

-
- [1] G.T. Horowitz, arXiv: 1002.1722 [hep-th].
 - [2] S.A. Hartnoll, Class. Quant. Grav. **26**, 224002 (2009).
 - [3] C.P. Herzog, J. Phys. A **42**, 343001 (2009).
 - [4] S.S. Gubser, Phys. Rev. D **78**, 065034 (2008).
 - [5] X.H. Ge, B. Wang, S.F. Wu, and G.H. Yang, J. High Energy Phys. **08**, 108 (2010).
 - [6] S. A. Hartnoll, C. P. Herzog and G. T. Horowitz, J. High Energy Phys. **0812**, 015 (2008).
 - [7] R. Gregory, S. Kanno and J. Soda, J. High Energy Phys. **0910**, 010(2009) [arXiv:0907.3203 [hep-th]].
 - [8] E. Nakano and W.Y. Wen, Phys. Rev. D **78**, 046004 (2008).
 - [9] I. Amado, M. Kaminski, and K. Landsteiner, J. High Energy Phys. **05**, 021 (2009).
 - [10] G. Koutsoumbas, E. Papantonopoulos, and G. Siopsis, J. High Energy Phys. **07**, 026 (2009).
 - [11] O.C. Umeh, J. High Energy Phys. **08**, 062 (2009).
 - [12] J. Sonner, Phys. Rev. D **80**, 084031 (2009).
 - [13] J.L. Jing and S.B. Chen, Phys. Lett. B **686**, 68 (2010).
 - [14] S. Franco, A.M. Garcia-Garcia, and D. Rodriguez-Gomez, Phys. Rev. D **81**, 041901(R) (2010).
 - [15] C.P. Herzog, Phys. Rev. D **81**, 126009 (2010); arXiv:1003.3278 [hep-th].
 - [16] G.T. Horowitz and M.M. Roberts, Phys. Rev. D **78**, 126008 (2008).
 - [17] R.A. Konoplya and A. Zhidenko, Phys. Lett. B **686**, 199 (2010).
 - [18] G. Siopsis and J. Therrien, J. High Energy Phys. **05**, 013 (2010).
 - [19] K. Maeda, M. Natsuume, and T. Okamura, Phys. Rev. D **79**, 126004 (2009).
 - [20] R.G. Cai, Z.Y. Nie, and H.Q. Zhang, Phys. Rev. D **82**, 066007, (2010).
 - [21] Q.Y. Pan, B. Wang, E. Papantonopoulos, J. Oliveria, and A.B. Pavan, Phys. Rev. D **81**, 106007 (2010).
 - [22] Q.Y. Pan and B. Wang, Phys. Lett. B **693**, 159, (2010).
 - [23] L. Barclay, R. Gregory, S. Kanno, and P. Sutcliffe, J. High Energy Phys. **12**, 029 (2010).
 - [24] M. Siani, J. High Energy Phys. **12**, 035 (2010); arXiv: 1010.0700 [hep-th].
 - [25] J. Jing, L.C. Wang, Q.Y. Pan and S.B. Chen, Phys. Rev. D **83**, 066010, (2011).
 - [26] R. Gregory, J. Phys. Conf. Ser. **283**(2011) 012016, arXiv:1012.1558.
 - [27] L. Barclay, arXiv:1012.3074 [hep-th].
 - [28] R.G. Cai, Z.Y. Nie, and H.Q. Zhang, Phys. Rev. D **83**, 066013, (2011).
 - [29] H.F. Li, R.G. Cai, and H.Q. Zhang, J. High Energy Phys. **04**, 028 (2011); arXiv:1103.2833 [hep-th].
 - [30] S. Kanno, Class. Quant. Grav. **28**, 127001 (2011); arXiv:1103.5022 [hep-th].
 - [31] Q.Y. Pan, J.L. Jing, and B. Wang, J. High Energy Phys. **11**, 088 (2011); arXiv:1105.6153 [gr-qc].
 - [32] M. R. Setare and D. Momeni, EPL, **96**, 60006, (2011) .
 - [33] R. G. Cai, H. Q. Zhang, Phys. Rev. D **81**, 066003, (2010).
 - [34] D. Momeni, M. R. Setare, N. Majd, J. High Energy Phys. **05**, 118(2011), arXiv:1003.0376.
 - [35] J. P. Wu, Y. Cao, X. M. Kuang, W.J. Li, Phys. Lett. B **697**, 153, (2011), [arXiv:1010.1929v3 [hep-th]]; D. Momeni, arXiv:1106.0431.
 - [36] D.J. Gross and J.H. Sloan, Nucl. Phys. B **291**, 41 (1987).
 - [37] R. G. Cai and Y. W. Sun, JHEP **0809**, 115 (2008) [arXiv:0807.2377 [hep-th]].
 - [38] Q. Pan, J. Jing and B. Wang, Phys. Rev. D **84**, 126020 (2011) [arXiv:1111.0714[gr-qc]].
 - [39] M. Born and L. Infeld, Proc. R. Soc. A **144**, 425 (1934).
 - [40] G. W. Gibbons and D. A. Rasheed, Nucl. Phys. B **454**, 185 (1995).
 - [41] Y.Q. Liu and B. Wang, arXiv:1111.6729 [hep-th].
 - [42] J.L. Jing, L.C. Wang, Q.Y. Pan, and S.B. Chen, Phys. Rev. D **83**, 066010 (2011).
 - [43] J.L. Jing, Q.Y. Pan and S.B. Chen, arXiv:1106.5181[hep-th].
 - [44] S. Gangopadhyay and D. Roychowdhury, arXiv:1111.6729 [hep-th].
 - [45] T. K. Dey, Phys. Lett. B **595**, 484 (2004).
 - [46] R. G. Cai, D. W. Pang and A. Wang, Phys. Rev. D **70**, 124034 (2004).
 - [47] D. Wiltshire, Phys. Rev. D **38**, 2445 (1988).
 - [48] O. Miskovic and R. Olea, Phys. Rev. D **83**, 024011, (2011).
 - [49] Y.Q. Liu, Q.Y. Pan, B. Wang, and R.G. Cai, Phys. Lett. B **693**, 343 (2010).
 - [50] B. Wang, C.Y. Lin, and E. Abdalla, Phys. Lett. B **481**, 79 (2000).
 - [51] J.M. Zhu, B. Wang, and E. Abdalla, Phys. Rev. D **63**, 124004 (2001).
 - [52] B. Wang, C. Molina, and E. Abdalla, Phys. Rev. D **63**, 084001 (2001).